Thermal Destabilization of Non-phosphorylating Glyceraldehyde-3-phosphate Dehydrogenase from Streptococcus mutans upon Phosphate Binding in the Active Site

Sophie Rahuel-Clermont, Denis Arutyunov, Stephane Marchal, Victor Orlov, Vladimir Muronetz, Guy Branlant

THE JOURNAL OF BIOLOGICAL CHEMISTRY
Vol. 280, No. 19, Issue of May 13, pp. 18590–18597, 2005
Printed in U.S.A.

Thermal Destabilization of Non-phosphorylating Glyceraldehyde-3-phosphate Dehydrogenase from *Streptococcus mutans* upon Phosphate Binding in the Active Site*

Received for publication, December 15, 2004, and in revised form, March 8, 2005
Published, JBC Papers in Press, March 9, 2005, DOI 10.1074/jbc.M414110200

Sophie Rahuel-Clermont‡§, Denis Arutyunov§¶, Stéphane Marchal‡‖, Victor Orlov¶, Vladimir Muronetz‡¶, and Guy Branlant‡**

From the ‡Unité Mixte de Recherche 7567 CNRS-Université Henri Poincaré, Maturation des ARN et Enzymologie Moléculaire, Faculté des Sciences, Université Henri Poincaré Nancy I, BP 239, 54506 Vandoeuvre-lès-Nancy Cedex, France, and the ¶Belozersky Institute of Physico-Chemical Biology, Moscow State University, 119992 Moscow, Russia

Catalysis by the NADP-dependent non-phosphorylating glyceraldehyde-3-phosphate dehydrogenase (GAPN) from *Streptococcus mutans*, a member of the aldehyde dehydrogenase (ALDH) family, relies on a local conformational reorganization of the active site. This rearrangement is promoted by the binding of NADP and is strongly kinetically favored by the formation of the ternary complex enzyme·NADP·substrate. Adiabatic differential scanning calorimetry was used to investigate the effect of ligands on the irreversible thermal denaturation of GAPN. We showed that phosphate binds to GAPN, resulting in the formation of a GAPN·phosphate binary complex characterized by a strongly decreased thermal stability, with a difference of at least 15 °C between the maximum temperatures of the thermal transition peaks. The kinetics of phosphate association and dissociation are slow, allowing both free and GAPN·phosphate complexes to be observed by differential scanning calorimetry and to be separated by native polyacrylamide electrophoresis run in phosphate buffer. Analysis of a set of mutants of GAPN strongly suggests that phosphate is bound to the substrate C-3 subsite. In addition, the substrate analog glycerol-3-phosphate has similar effects as does phosphate on the thermal behavior of GAPN. Based on the current knowledge on the catalytic mechanism of GAPN and other ALDHs, we propose that ligand-induced thermal destabilization is a mechanism that provides to ALDHs the required flexibility for an efficient catalysis.

Non-phosphorylating glyceraldehyde-3-phosphate dehydrogenase (GAPN)[1] (EC 1.2.1.9) catalyzes the irreversible, NADP-dependent oxidation of D-glyceraldehyde-3-phosphate (D-GAP) into 3-phosphoglycerate. It belongs to the widely distributed aldehyde dehydrogenase (ALDH) superfamily, which participates in many levels of the cellular metabolism in the three kingdoms. As an enzyme involved in the production of NADPH equivalents required in biosynthetic pathways, GAPN is found in photosynthetic and non-photosynthetic cells of higher plants, photosynthetic microorganisms, and some eubacteria, such as certain strains of *Streptococci* (1, 2). GAPN from *Streptococcus mutans* catalyzes the oxidation of D-GAP via a two-step mechanism, following an ordered sequential mechanism, with NADP acting as the first binding substrate and D-GAP as the second binding substrate. At high concentration, D-GAP behaves as a competitive substrate inhibitor, thus indicating that GAP can bind to the apoenzyme (3). In the acylation step, a covalent thiohemiacetal intermediate is formed with the catalytic residue Cys-302, preceding the oxidoreduction process that leads to a thioacyl intermediate and formation of NADPH. The deacylation step includes the attack of a water molecule on the thioacyl intermediate and the release of 3-phosphoglycerate and NADPH.

Previous enzymatic and structural studies have highlighted the importance of ligand binding and local reorganization of the active site in the mechanism, affording high catalytic efficiency to GAPN. Specifically, the binding of NADP induces a local conformational rearrangement that leads to the accessibility of the thiol of Cys-302, combined to a shift of pK_{app} from 8.5 to 6.2, and a positioning adapted to subsequently form the competent thiohemiacetal intermediate. This rearrangement of the GAPN·NADP binary complex is strongly kinetically favored when the ternary complex enzyme·cofactor·substrate is formed (4). In addition, the side chains of Glu-268 and Arg-459 rotate, thus leading to the breaking of the ionic bridge that exists in the Apo1 crystal form (see next paragraph). At this point, the side chain of Arg-459 is orientated toward the substrate binding site. During this rearrangement, the distance between the functional groups of Glu-268 and Cys-302 decreases from 7.6 to 3.6 Å. Concomitantly, the oxyanion hole is formed, comprising at least the amide side chain of Asn-169 and the main chain amide of Cys-302, and is postulated to be responsible for the stabilization of the tetrahedral transition states produced during the acylation and deacylation steps (3, 4, 5). In this latter step, the side chain of Glu-268 has been shown to be responsible for the activation of the water molecule involved in the

* This research was supported by the Centre National de la Recherche Scientifique, the University Henri Poincaré Nancy I, the IFR 111 Bioingénierie and by the Russian Foundation of Basic Research (Grant 02–04-8076). The costs of publication of this article were defrayed in part by the payment of page charges. This article must therefore be hereby marked "*advertisement*" in accordance with 18 U.S.C. Section 1734 solely to indicate this fact.

§ Both authors contributed equally to this work.

‖ Present address: Equipe d'accueil 3763, Université Montpellier 2, CC 105 Place Eugène Bataillon, 34095 Montpellier cédex 5, France.

** To whom correspondence should be addressed: UMR 7567 CNRS-UHP, Maturation des ARN et Enzymologie Moléculaire, Faculté des Sciences, Université Henri Poincaré Nancy I, BP 239, 54506 Vandoeuvre-lès-Nancy Cedex, France. Tel.: 33-383-68-43-04; Fax: 33-383-68-43-07; E-mail: guy.branlant@maem.uhp-nancy.fr.

[1] The abbreviations used are: GAPN, non-phosphorylating glyceraldehyde-3-phosphate dehydrogenase; ALDH, aldehyde dehydrogenase; CD, circular dichroism; DSC, differential scanning calorimetry; GAP, glyceraldehyde-3-phosphate; G3P, DL-α-glycerophosphate (glycerol-3-phosphate); DTNB, 5,5′-dithiobis(2-nitrobenzoic acid); TES, *N*-tris(hydroxymethyl)methyl-2-aminoethanesulfonic acid; T_{max}, maximum temperature of the thermal transition peak.

hydrolysis of the thioacyl intermediate (3). Recent studies on human cytosolic and mitochondrial ALDHs have suggested an isomerization event of the nicotinamide mononucleotide moiety of the cofactor, which would be required for Glu-268 to play this role in the deacylation step (6, 7).

Three sulfate binding sites have been described in the crystal structures of the apoforms of GAPN obtained so far, which provided bases for the characterization of the ligand binding sites (5, 8). The first one, the SO_4a site, exists both in Apo1 and Apo2 forms of GAPN and includes Arg-124 and Arg-301 side chains and Arg-459 and Gly-460 main-chain amide groups. In the Apo1 structure, Arg-459 and Glu-268 side chains interact via an ionic bridge, which is split in the Apo2 structure. The second sulfate site, the SO_4b site, has only been found in the Apo2 structure and is shaped by Arg-301 and Arg-459 guanidinium groups, Asn-169 side-chain and Cys-302 and Thr-303 main-chain amide groups. The Thr-303 residue also interacts with the sulfate ions in both sites through the hydroxyl group of its side chain. The sulfate anion bound in the SO_4b site most likely mimics the tetrahedral transition states of the substrate C-1 involved in the acylation and deacylation steps. A systematic study of the role of these arginine residues led to the conclusions that Arg-124 is only involved in stabilizing D-GAP binding via an interaction with the C-3 phosphate, and the Arg-301 side chain and Arg-459 main chain participate, not only in D-GAP binding via interaction with C-3 phosphate, but also in positioning efficiently D-GAP relative to Cys-302 within the ternary complex GAPN·NADP·GAP (9). The third sulfate site corresponds to the subsite of the 2′-phosphate group of the adenosine part of NADP and comprises residues Lys-192 and Thr-195 side chains (10, 11).

The role of ligand interactions on the structure of the active site, as revealed by enzymatic, biochemical, and structural approaches, raises the question of the identification and characterization of such interactions and of their potential catalytic significance. In this work, we used the thermal unfolding of GAPN followed by adiabatic differential scanning calorimetry (DSC) to investigate the relationships between thermal stability and active site interactions of GAPN with ligands, with respect to the catalytic mechanism.

EXPERIMENTAL PROCEDURES

Materials, Site-directed Mutagenesis, Production, and Purification of Wild-type and Mutant Enzymes—Production and purification procedures were carried out as described previously (4). The purification process was carried out in 50 mM potassium inorganic phosphate buffer, pH 6.4. Site-directed mutageneses were performed using the method of Kunkel *et al.* (12) or the QuikChange site-directed mutagenesis kit (Stratagene). The enzymes were isolated as the apoform, judging by the absorbance ratio A_{280}/A_{260} of 2.0 and by the fact that no NADP was enzymatically detectable after acidic denaturation. In the text, GAPN will therefore refer to apoGAPN. Enzyme purity was checked by SDS-PAGE analysis using 7.5% resolving gel. The GAPN monomer concentration was estimated spectrophotometrically at 280 nm, using an extinction coefficient of $5.01 \times 10^4\ M^{-1}\cdot cm^{-1}$, as deduced by the method of Scopes (13). Subunit molecular mass (~51 kDa) of wild-type and mutant GAPNs were checked by mass spectrometry. For all experiments described, the samples of GAPN were stored in saturated ammonium sulfate in 50 mM potassium P_i buffer, pH 6.4, at −20 °C and were desalted by gel filtration, either on a Sephadex G-25 column or an Econo-Pac 10 DG polyacrylamide gel column (Bio-Rad), or dialyzed for at least 20 h against the appropriate buffer before the experiments. Both gel filtration and dialysis procedures gave very similar DSC results. The activity of the enzyme was not significantly affected by the sample preparation.

All other materials were reagent grade or better and were used without further purification. Potassium P_i was from BDH, NADP was from Roche Applied Science, and DTNB and G3P were from Sigma. DL-GAP (Sigma) was hydrolyzed from DL-GAP diethylacetal according to the manufacturers' instructions and enzymatically titrated with GAPN.

Enzyme Kinetics—Initial rate measurements were carried out at 25 °C spectrophotometrically by following the appearance of NADPH at 340 nm. Because GAPN is equally active with the D and L isomers of GAP, DL-GAP was used for activity measurements. The standard experimental conditions were 1 mM NADP, 0.2 mM DL-GAP, 50 mM TES buffer, 5 mM β-mercaptoethanol, pH 8.2. The competitive inhibition constant of G3P for GAP was determined under conditions where GAP does not significantly behave as a competitive substrate inhibitor, *i.e.* below 0.2 mM (3).

Differential Scanning Calorimetry—Differential scanning calorimetry measurements were made using a DASM-4 adiabatic microcalorimeter (Biopribor, Poushchino, Russia) with 0.47-ml platinum capillary spiral cells at excessive pressure of 2 atmospheres as described previously (14, 15). The calorimetric reversibility of the thermally induced transitions was checked by reheating the protein solution in the calorimeter after cooling from the first run, stopped at the end of the transition (*i.e.* ~55 and ~80 °C for transition B and A, respectively, see "Results"). Temperature scanning rates (ν) of 1.5, 1.0, 0.5, and 0.2 °C/min were tested. Subsequently, most experiments in this study were performed at a constant scan rate of 1 °C/min. The thermograms were recorded in the range of 0.1–1.2 mg/ml protein. Instrumental baselines recorded with both cells filled with buffer were subtracted from the experimental traces to obtain the heat capacity curves (ΔCp, excess heat capacity, *versus* temperature). Original software was used for recording the DSC data, and MicroCal Origin versions 1.16 and 7.0 were used to determine the T_{max} (maximum of the thermal transition peak) and calorimetric enthalpies (ΔH_{cal}) values. For ionic strength controls and kinetic experiments, DSC was performed on a Microcal VP-DSC apparatus equipped with cylindrical 0.54-ml cells under identical conditions, except for the protein concentration fixed at 0.1–0.2 mg/ml. The T_{max} and ΔH_{cal} values measured on thermograms obtained with both calorimeters under the same conditions were very similar. Because of the irreversibility of the heat denaturation process, it was impossible to calculate the value of the van't Hoff enthalpy.

CD Spectroscopy—Circular dichroism (CD) spectra of GAPN (0.1 mg/ml) were recorded on a Jobin-Yvon CD6 spectropolarimeter using dedicated software. Measurements were recorded in a quartz cuvette with a 1-mm path length at 25 and 55 °C. Spectra were recorded as an average of six to eight scans from 205 to 260 nm.

Gel Filtration—Gel filtration experiments were carried out on a Superose 12 HR 10/30 column using a Pharmacia Corporation fast protein liquid chromatography system at room temperature. Protein (4.9 μM) in a 200-μl aliquot was applied onto the column equilibrated with 50 or 250 mM potassium P_i buffer, pH 8.2, at 25 °C. The flow rate was 0.5 ml/min, and the protein was detected spectrophotometrically at 280 nm. Thyroglobulin (670 kDa), bovine globulin (158 kDa), chicken ovalbumin (44 kDa), horse myoglobin (17.5 kDa), and vitamin B_{12} (1.35 kDa) were used as references to calibrate the column.

Analytical Ultracentrifugation—Sedimentation of GAPN was studied using a model E Spinco analytical ultracentrifuge (Beckman-Spinco) equipped with a photoelectric scanner, a multiplexer, and a monochromator. An analytical titanium rotor Model F and double-sector cells were used. UV light scanning was carried out at 280 nm. The sedimentation studies were performed at 25 and 45 °C and 261,600 × *g* in 50 or 250 mM potassium P_i buffer, pH 8.2. The sedimentation coefficients were normalized to the standard conditions, *i.e.* a solvent with the density and viscosity of water at 20 °C. Before both gel filtration and ultracentrifugation experiments, GAPN samples were desalted in the indicated buffers by gel filtration from the stock suspension in saturated ammonium sulfate in 50 mM potassium P_i buffer, pH 6.4.

Native PAGE—Mini Protean 3 cell (Bio-Rad) was used for native PAGE analyses in 8% acrylamide gel (with 2.67% methylene-bis-acrylamide). The temperature of the cell was regulated to 4 °C to avoid overheating. The samples were desalted by gel filtration from the stock suspension in saturated ammonium sulfate into the appropriate running buffer (pH 8.2) prior to the experiment. A voltage of 50 V was used for 1.5 h for gels run in potassium P_i buffers, pH 8.2, and 100 V for 1 h for gels run in 80 mM Tris-glycine buffer, pH 8.2.

Inorganic Phosphate Determination—The C302A GAPN was desalted from the ammonium sulfate stock suspension in 50 mM potassium P_i buffer, pH 6.4, by gel filtration in 50 mM ammonium acetate buffer, pH 8.2, or eluted with water from polyacrylamide gel after native PAGE in 80 mM Tris-glycine, pH 8.2, and then precipitated using trifluoroacetic acid before phosphate determination in the supernatant, according to Van Veldhoven *et al.* and Cogan *et al.* (16, 17). Briefly, the method is based on the formation of phosphomolybdate complexes revealed by interaction with malachite green under acidic conditions in the presence of polyvinyl alcohol to stabilize the interaction. Ammo-

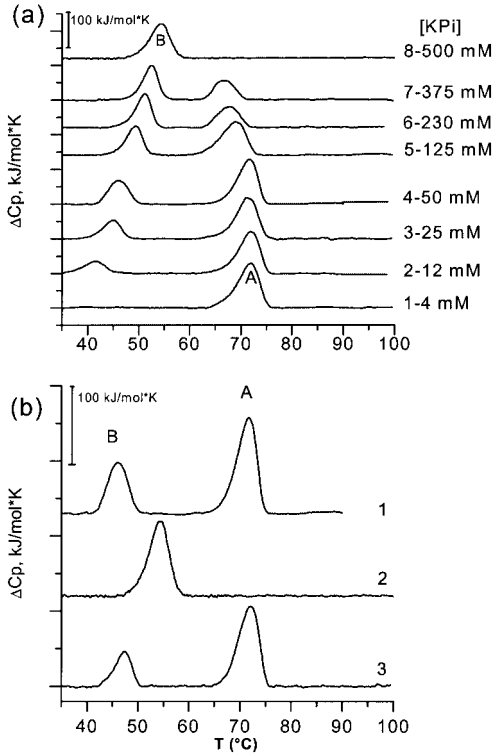

FIG. 1. **Analysis of the effect of phosphate concentration on the thermal unfolding of wild-type GAPN followed by DSC.** The enzyme (0.5 mg/ml) stored as ammonium sulfate precipitate was dialyzed for at least 20 h against potassium P_i buffers, pH 8.2. *a*, *curves 1–8*, effect of increasing potassium P_i (*KPi*) concentration from 4, 12, 25, 50, 125, 250, and 375 to 500 mM, respectively. Components A and B of the thermograms are indicated (see "Results"). *b*, the reversibility of the effect of phosphate anions. Wild-type GAPN in 500 mM potassium P_i (*curve 2*) was dialyzed for 20 h against 50 mM potassium P_i buffer, pH 8.2 (*curve 3*). The thermogram of the enzyme in 50 mM potassium P_i, pH 8.2 (*curve 1*) is shown for comparison. *T*, temperature.

nium heptamolybdate in 7.30 N H_2SO_4 was added at 0.29% (w/v) final concentration, incubated for 10 min at 25 °C, followed by a mixture of malachite green (0.005% (w/v) final) and polyvinyl alcohol (0.05% (w/v) final). After 30 min of incubation at 25 °C, absorbance was measured at 610 nm. At least three independent experiments were performed for each determination.

Accessible Cysteine Content in Enzyme Preparations Measured with DTNB—The amount of reacted cysteines was deduced from the absorbance of thionitrobenzoate released after reaction with DTNB using an extinction coefficient of 13 600 $M^{-1} \cdot cm^{-1}$ at 412 nm. The enzyme was desalted in 50 mM potassium P_i buffer, pH 8.2, before adding the sulfhydryl reagent in large excess relative to the enzyme and following the reaction at 25 °C.

RESULTS

The Thermal Denaturation of Wild-type GAPN in the Presence of Phosphate—The thermal behavior of GAPN was first studied by DSC at a scan rate of 1 °C/min in the presence of increasing concentrations of potassium P_i at pH 8.2. As shown in Fig. 1*a*, the thermograms of GAPN revealed two endotherms showing T_{max} values differing by at least 15 °C (15–30 °C), referred to as A and B for the high and low temperature transitions, respectively. Increasing potassium P_i concentration resulted in an increase of the area of endotherm B at the expense of that of endotherm A, with a concomitant increase of T_{max} from 41.9 to 54.7 °C. Conversely, at high potassium P_i concentrations (>125 mM), the T_{max} of endotherm A tended to decrease from 72 to 67 °C. At 500 mM potassium P_i, the "conversion" of endotherm A into endotherm B was complete. Decreasing the potassium P_i concentration from 500 to 50 mM by extensive dialysis (for 20 h, see "Kinetics of the GAPN-Phosphate Interaction") restored the GAPN thermogram back to the initial observation in 50 mM potassium P_i (Fig. 1*b*).

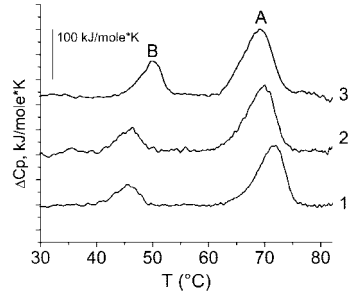

FIG. 2. **Effect of the ionic strength on the thermal unfolding of wild-type GAPN followed by DSC.** Thermograms were recorded in 50 mM potassium P_i, pH 8.2 (*curve 1*), 300 mM NaCl in 50 mM potassium P_i, pH 8.2 (*curve 2*), and 150 mM potassium P_i, pH 8.2 (*curve 3*). The enzyme from the ammonium sulfate precipitate stock suspension in 50 mM potassium P_i buffer, pH 6.4, was dialyzed for at least 20 h in the indicated buffers before the experiment. The protein concentration was 0.1 mg/ml. *T*, temperature.

To test whether the observed phenomenon corresponded to a specific or a nonspecific ionic strength-dependent interaction between phosphate ions and GAPN, the effect of the presence of 300 mM NaCl in a solution of GAPN in 50 mM potassium P_i was compared with the effect of phosphate at the similar ionic strength of ~0.45 M in 150 mM potassium P_i. As shown on Fig. 2, NaCl does not affect significantly the characteristics of endotherm B, whereas higher potassium P_i concentration increases both the area and T_{max} of the endotherm. The T_{max} of endotherm A was decreased in the presence of increased potassium P_i or NaCl concentration at fixed ionic strength. Higher concentrations of NaCl (up to 1.35 M) added to 20 mM potassium P_i solutions, which lead to ionic strength values of up to ~1.5 M (corresponding to 500 mM potassium P_i, pH 8.2), resulted in similar effects either on endotherm B (no significant effect) or on endotherm A (decrease of T_{max}) (data not shown).

Both B and A thermal transitions were irreversible and scan rate-dependent. Decreasing the scanning rate from 1.5 to 0.2 °C/min resulted in a shift of T_{max} toward lower temperatures (Fig. 3). Analysis of the scan rate dependence of the wild-type GAPN thermogram in 50 mM potassium P_i showed the non-saturating, linear dependence of T_{max} as a function of scan rate, suggesting kinetically controlled processes for both transitions (18, 19)(curves not shown). The agreement of the mechanism of thermal unfolding to a simple first-order kinetic model was checked according to the criteria developed by Kurganov *et al.* (20). For scan rates 0.5–1.5 °C/min, good superpositioning of the ln ΔCp *versus* $1/T$ and $1/T$ *versus* $\ln(\nu\Delta Cp/(\Delta H_{cal} - \Delta H(T)))$ profiles for transition A (with $\Delta H(T)$, corresponding to the denaturation heat capacity at temperature *T*) suggests that the unfolding mechanism of GAPN that gives rise to this transition is very close to a simple first-order process (curves not shown). Determination of the apparent activation energy of transition A according to different methods described by Sanchez-Ruiz *et al.* (18) gave consistent values, with an average of 454 ± 3 kJ/mol. Similar analysis for the B transition revealed deviations from the simple model, suggesting the involvement of intermediates in the unfolding mechanism (curves not shown). Nevertheless, an approximate mean value of 441 ± 6 kJ/mol could be determined for the activation energy of this transition.

Due to the irreversible nature of the thermal denaturation process, the ΔH_{cal} values for both transitions likely are not strictly proportional to each species concentration, because they can be affected by the mechanism of irreversible thermal unfolding. This precluded a rigorous quantitative analysis of

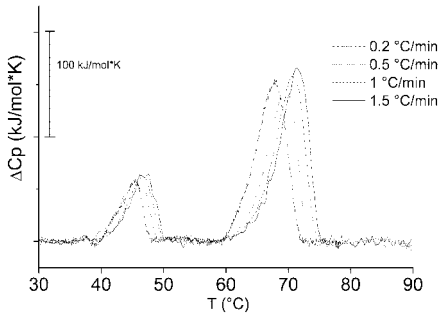

FIG. 3. **Effect of the scanning rate on the thermograms of wild-type GAPN.** Thermograms were recorded in 50 mM potassium P_i, pH 8.2, at a scan rate of 1.5 (*solid line*), 1 (*dashed line*), 0.5 (*dotted line*) and 0.2 (*dashed/dotted line*) °C/min. The enzyme was dialyzed from the ammonium sulfate stock suspension in 50 mM potassium P_i, pH 6.4, for at least 20 h in the buffer before the experiment. The protein concentration was 0.2 mg/ml. *T*, temperature.

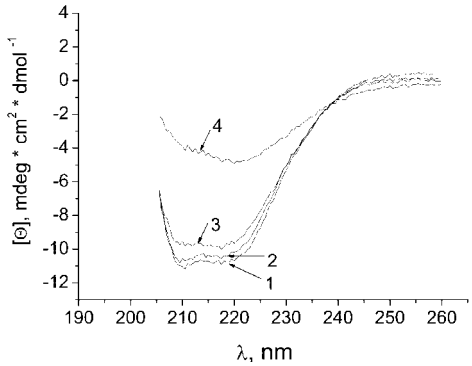

FIG. 4. **Circular dichroism spectra of wild-type GAPN.** (0.1 mg/ml) recorded at 25 °C in 10 mM (*curves 1* and *3*) and 500 mM (*curves 2* and *4*) potassium P_i buffer, pH 8.2, before (*curves 1* and *2*) and after (*curves 3* and *4*) 20 min of incubation at 55 °C. The samples were desalted from the stock suspension in saturated ammonium sulfate into the appropriate buffer by gel filtration prior to the experiment.

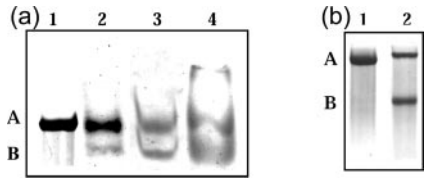

FIG. 5. **Native PAGE profiles of GAPN at pH 8.2.** *a*, native PAGE analyses of wild-type GAPN (3 μg, *lanes 1–4*) were run in 4, 12, 50, and 250 mM potassium P_i buffer, respectively. *b*, native PAGE analyses of wild-type (5 μg, *lane 1*) and C302A GAPNs (5 μg, *lane 2*) were run in 80 mM Tris-glycine buffer. The samples were desalted from the stock suspension in saturated ammonium sulfate in 50 mM potassium P_i buffer, pH 6.4, into the appropriate running buffer, pH 8.2, by gel filtration prior to the experiment.

the DSC data, which were used only to provide estimates of the kinetics of the processes observed, required for this study.

Endotherms A and B Correspond to Two Species of Tetrameric GAPN—Regarding the origin of transitions A and B, the latter could result from the dissociation of the GAPN tetramer into subunits. However, the following experiments excluded this assumption. First, neither the A nor the B transitions were dependent on the protein concentration, indicating that the rate-limiting step of the thermally induced processes occurs prior to the dissociation of the subunits. Second, gel filtration on Superose 12 in the presence of 50 and 250 mM potassium P_i buffer, pH 8.2, showed only one peak corresponding to a molecular weight of ~200,000 at 25 °C (curve not shown). Third, only one type of species with a sedimentation coefficient ($S_{w,20}$) of 8.32 ± 0.27 S, corresponding to a molecular weight of ~200,000, was shown from sedimentation experiments run in 50 and 250 mM potassium P_i buffer, pH 8.2, at 25 and 45 °C, respectively. Altogether, these experiments showed that endotherms A and B observed in the presence of phosphate correspond to two species of tetrameric GAPN.

The thermal destabilization of GAPN upon increase of the potassium P_i concentration was further studied by far-UV CD analysis. For GAPN samples containing 10 and 500 mM[2] potassium P_i, pH 8.2, respectively, CD spectra showed similar profiles, thereby indicating that high concentrations of potassium P_i do not significantly affect the secondary structure content of GAPN (Fig. 4, *curves 1* and *2*). In contrast, after heating at 55 °C for 20 min, drastic changes were observed in the CD profile of the sample containing 500 mM potassium P_i, pH 8.2, as shown by the loss of the content of the secondary structures (Fig. 4, *curve 4*). The minor changes occurring after thermal treatment of GAPN under the same conditions in the presence of 10 mM potassium P_i, pH 8.2, are thus roughly consistent with the loss of the amount of the thermolabile species existing at this concentration (Fig. 1 and Fig. 4, *curve 3*).

Finally, two well separated bands were revealed by native PAGE of GAPN solutions run in potassium P_i buffers, pH 8.2 (Fig. 5*a*). In the presence of increasing concentration of potassium P_i from 4 to 250 mM, the slower-migrating band became relatively less abundant compared with the faster one. Altogether, this result combined to the DSC and CD data suggests that 1) the slower-migrating band corresponds to the species unfolding in transition A by DSC and 2) phosphate binds to GAPN, resulting in the formation of a GAPN·phosphate binary complex characterized by a lower thermostability (thermal unfolding transition B) and a higher electrophoretic mobility than the unliganded GAPN species.

Phosphate Content in C302A GAPN—To titrate the phosphate content of both GAPN species, the PAGE technique in a buffer devoid of phosphate (*i.e.* 80 mM Tris-glycine, pH 8.2) appeared as a method of choice to isolate the two forms, provided that the kinetics of phosphate dissociation were slow enough compared with the timescale of the PAGE separation (see "Kinetics of the Phosphate-GAPN Interaction"). Attempts to visualize a band corresponding to the faster-migrating band in samples of wild-type GAPN were unsuccessful. Only one slower-migrating band was seen under these conditions. In contrast, under the same conditions, two bands were visualized for C302A GAPN (Fig. 5*b*). Therefore, the phosphate content was investigated on each band of C302A GAPN using a colorimetric method based on the interaction of malachite green with phosphomolybdate complexes.

First, the phosphate content in the C302A enzyme sample was determined after desalting from the stock suspension as ammonium sulfate precipitate in 50 mM potassium P_i buffer, pH 6.4, through a Sephadex G-50 column equilibrated with 50 mM ammonium acetate buffer, pH 8.2. Under these conditions, 1 mol of C302A GAPN tetramer contained an average of 1.36 ± 0.09 mol of phosphate. Second, in a separate experiment, the same sample of C302A GAPN was migrated on PAGE run in 80 mM Tris-glycine buffer, pH 8.2. Strips corresponding to each band were cut, and the phosphate content was determined in each band after elution, followed by protein precipitation. Only the strip corresponding to the faster-migrating band contained phosphate, with a stoichiometry of 3.8 ± 0.4 mol/mol of GAPN tetramer, which strongly suggested

[2] A low concentration of phosphate is required to maintain the full activity of GAPN. Indeed, in the absence of phosphate, *e.g.* in Tris-glycine buffer, GAPN is transformed into the inactive GAPN* form (see "Results").

a stoichiometry of 1 phosphate/C302A mutant GAPN subunit. This result, which can reasonably be extrapolated to the phosphate content of the wild-type enzyme, even though the faster-migrating band could not be isolated in the wild type under the conditions used, again supports the existence of a GAPN·phosphate binary complex.

Kinetics of the GAPN-Phosphate Interaction—To get insight into the influence of the dynamics of the interaction on the timescale of the DSC and PAGE experiments, we measured the evolution of the endotherm B area in solutions of wild-type and C302A GAPNs prepared in 500 mM potassium P_i, pH 8.2 (as described under "Experimental Procedures"), dialyzed as a function of time against a 4 mM concentration of the same buffer at 4 °C. The data were analyzed as first-order kinetics (curves not shown) to provide estimates for the rate constants of 0.4 ± 0.1 and 0.011 ± 0.003 h^{-1} ($t_{1/2}$ of 1.7 and 63 h) for wild-type and C302A GAPNs, respectively. Similarly, the kinetics of appearance of the endotherm B were followed by the evolution of endotherm B area in solutions of wild-type GAPN prepared in 4 mM potassium P_i, pH 8.2, dialyzed for increasing time against 500 mM of the same buffer. The rate constant of the process was estimated to 0.3 ± 0.1 h^{-1} for wild-type GAPN ($t_{1/2}$ of 2.3 h). In addition, when a sample of wild-type GAPN was dialyzed from the stock suspension (in saturated ammonium sulfate in potassium P_i buffer, pH 6.4) against 4 mM potassium P_i buffer, pH 8.2, as a function of time, the DSC analysis revealed that at least a 20-h dialysis was necessary to complete the B→A transformation. Therefore, these conditions were used to prepare GAPN samples in most experiments in this study (see "Experimental Procedures").

Analysis of Mutant GAPNs—As mentioned in the Introduction section, x-ray structures of GAPN showed that three sulfate ions from the crystallization medium can bind to apoGAPN (5, 8). To identify which site bound the phosphate in the GAPN·phosphate binary complex, the thermograms of various mutants of GAPN were recorded under conditions where phosphate concentrations were not saturating. As shown in Fig. 6*a*, *curves 2–6*, two endotherms were visualized on the DSC profiles of N169T, T195G, E268A, C302A, and R459I GAPNs in the presence of 50 mM potassium P_i, pH 8.2. Compared with the wild type (Fig. 6*a*, *curve 7*), the amount of the thermolabile species was similar in T195G GAPNs, higher in C302A GAPN, but significantly lower in E268A, R459I, and N169T GAPNs. Only the R124L GAPN (Fig. 6*a*, *curve 1*) lacked endotherm B at 50 mM potassium P_i, whereas at 500 mM, a faint labile peak appeared. When desalted from saturated ammonium sulfate in 80 mM Tris-glycine buffer, pH 8.2, the R124L, N169T, T195G, E268A, R459I, and the wild-type GAPNs lacked endotherm B (thermograms not shown). In contrast, under the same conditions, the C302A GAPN sample displayed two endotherms (Fig. 6*b*), in accordance with the results observed in the PAGE experiments (Fig. 5*b*). Profiles obtained on native PAGE using 50 mM potassium P_i, pH 8.2, as the running buffer were also determined (Fig. 6*c*). As previously mentioned, two well separated bands were seen under these conditions for wild-type GAPN. Similar to the wild type, N169T and R459I GAPNs exhibited two bands, whereas only one band was visualized for R124L GAPN.

Given the behavior of GAP, which has been shown to bind to apoGAPN, it was interesting to determine the DSC profile of GAPN in the presence of a high concentration of GAP. Unfortunately, under the DSC temperature conditions, GAP is not stable. Consequently, the DSC profile of wild-type GAPN was determined in the presence of 250 mM DL-α-glycerophosphate (G3P), which was shown to behave as a competitive inhibitor toward GAP (K_I = 16 ± 2 mM, data not shown) and had the

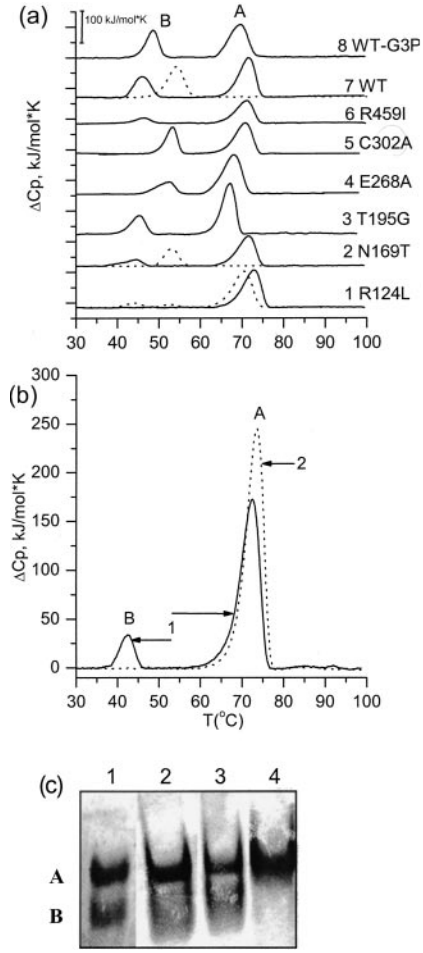

FIG. 6. **Analysis of the effect of various mutations on the thermal unfolding of the GAPN protein followed by DSC.** *a*, thermal unfolding followed by DSC (*curves 1–7*) of R124L, N169T, T195G, E268A, C302A, R459I, and wild-type (*WT*) GAPNs (1 mg/ml), respectively, in 50 mM (*solid lines*) and 500 mM (*dotted lines*, for R124L, N169T, and wild-type GAPN) potassium P_i buffer, pH 8.2. *Curve 8* corresponds to the thermogram of wild-type GAPN (1 mg/ml) in 4 mM potassium P_i buffer, pH 8.2, in the presence of 250 mM G3P. *b*, thermograms of C302A GAPN (*curve 1*, *solid line*) and wild-type (*curve 2*, *dotted line*) GAPNs (1 mg/ml) in 80 mM Tris-glycine buffer, pH 8.2. *T*, temperature. *c*, native PAGE analysis of the wild-type (5 μg, *lane 1*) and N169T, R459I, and R124L GAPNs (5 μg, *lanes 2–4*) in 50 mM potassium P_i, pH 8.2. All samples were dialyzed in the appropriate buffer, pH 8.2, for at least 20 h from the stock suspension in potassium P_i 50 mM/saturated ammonium sulfate prior to the experiment.

advantage of being chemically stable under the experimental conditions used. As shown in Fig. 6*a*, *curve 8*, two endotherms were visualized at pH 8.2 in 4 mM potassium P_i, pH 8.2, under conditions where no significant thermal transition B is detected by DSC in the absence of G3P (Fig. 1*a*, *curve 1*).

Selectivity of the Anion Binding Site in Wild-type GAPN—To determine the selectivity of the anion binding site in GAPN, DSC thermograms of solutions of GAPN in 20 mM potassium P_i, pH 8.2, were carried out in the presence of other anions at a fixed concentration of 480 mM. As shown in Fig. 7, in accordance with previous experiments shown in Fig. 2, chloride had no significant effect on the area and T_{max} of endotherm B. In contrast, sulfate induced the increase of the T_{max} and area of endotherm B in a similar manner as phosphate, except that a significant fraction of endotherm A remained. Compared with phosphate 20 mM, the addition of chloride and sulfate resulted in a thermal destabilization of the species unfolding as transition A.

Characterization of an Inactive Thermostable Species of Wild-type GAPN—Preliminary experiments, which consisted of

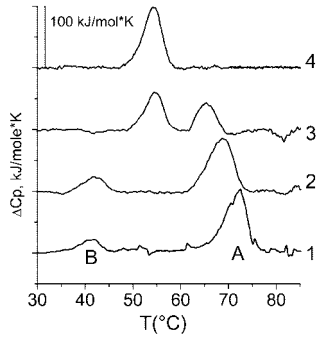

FIG. 7. **Effect of sulfate and chloride anions on the thermal unfolding of wild-type GAPN followed by DSC.** Salts (final concentration, 480 mM) were added to 20 mM potassium P_i, pH 8.2, and the enzyme was dialyzed for 20 h against these buffers before the DSC experiment. Thermograms of wild-type GAPN (0.1 mg/ml) were recorded in 20 mM potassium P_i, pH 8.2 (*curve 1*), 480 mM NaCl in 20 mM potassium P_i, pH 8.2 (*curve 2*), 480 mM ammonium sulfate in 20 mM potassium P_i, pH 8.2 (*curve 3*). The thermogram of GAPN in 500 mM potassium P_i, pH 8.2, is added for comparison (*curve 4*). *T*, temperature.

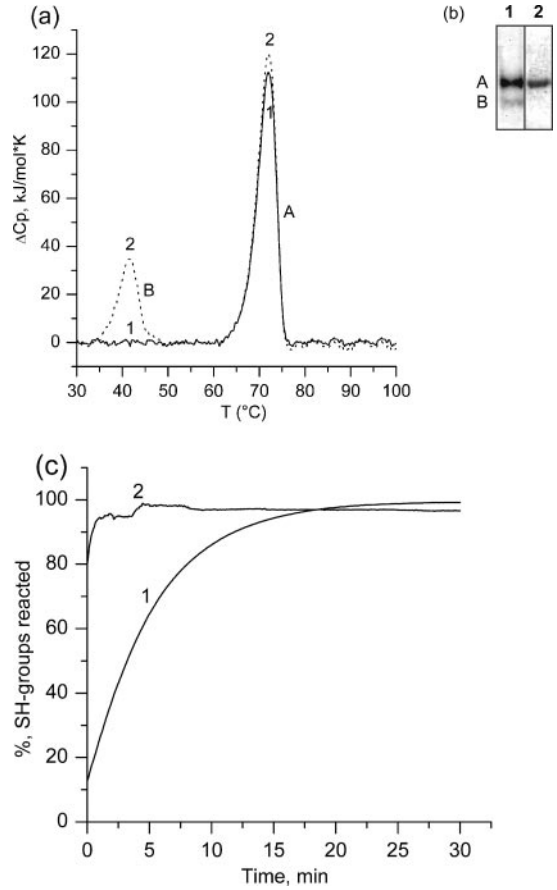

FIG. 8. **Analysis of the effect of 55 °C heating on wild-type GAPN solutions.** *a*, the thermogram of GAPN (1 mg/ml, *curve 1*, *solid line*) was recorded by DSC in 12 mM potassium P_i buffer, pH 8.2, after heating to 55 °C in the cell of the calorimeter from 20 to 55 °C at 1 °C/min followed by cooling to 20 °C. The thermogram of non-heated GAPN in the same buffer is shown for comparison (*curve 2*, *dotted line*). *T*, temperature. *b*, native PAGE profile of GAPN (3 μg) in 12 mM potassium P_i buffer, pH 8.2, before (*lane 1*) and after 20 min heating at 55 °C (*lane 2*). The smaller intensity of bands in *lane 2* might be due to the thermal denaturation and precipitation of a small fraction of protein during the heating step. *c*, titration by DTNB of cysteine residues of GAPN (1 mg/ml) in 12 mM potassium P_i buffer, pH 8.2, before (*curve 1*) and after (*curve 2*) 20 min heating at 55 °C. The ordinate full scale (100%) corresponds to two cysteines titrated/GAPN monomer.

heating GAPN (0.1 mg/ml) at 55 °C in 10 mM potassium P_i, pH 8.2, during 20 min showed that the enzyme had lost its activity, although its content in secondary structures did not significantly change, as shown from CD spectra (Fig. 4). This suggested that, under these heating conditions, the free GAPN was transformed into another form referred to as GAPN*. This was confirmed by experiments that suggested that the GAPN* was not capable of binding phosphate under the same conditions as GAPN. As an example, when a sample of GAPN (1 mg/ml) in 12 mM potassium P_i, pH 8.2 (conditions under which the major species of GAPN is in the non-complexed state) was exposed to a temperature increase from 20 to 55 °C at a constant scan rate of 1 °C/min, followed by cooling to 20 °C and then subjected to a full temperature scan, an endotherm with a T_{max} similar to that of endotherm A was revealed, whereas no endotherm corresponding to the thermolabile species was observed (Fig. 8*a*). Therefore, the endotherm of GAPN* corresponded to a GAPN species that had lost the capability of binding phosphate, even on the timescale of up to 24 h. Native PAGE profile confirmed the DSC analysis of the preheated sample. Only one band, which migrated in a similar manner to that of the band corresponding to the thermostable species (slow-migrating band), was observed when the native PAGE was run in 12 mM potassium P_i buffer, pH 8.2 (Fig. 8*b*).

To get more structural information on the different tetrameric GAPN species, the reactivity of cysteines was investigated. In wild-type GAPN, two cysteines (Cys-302 in the active site and Cys-382 located on the surface of the tetramer) are titratable by DTNB (4). In GAPN in 12 mM potassium P_i pH 8.2, *i.e.* in conditions under which the main GAPN species is the unliganded one, both cysteines are poorly accessible and thus react slowly (Fig. 8*c*, *curve 1*). Under high potassium P_i concentration, in conditions where the major species corresponds to the GAPN·phosphate complex, the cysteines remained poorly accessible (data not shown). By contrast, as shown in Fig. 8*c*, when wild-type GAPN (1 mg/ml) in 12 mM potassium P_i buffer, pH 8.2, was heated at 55 °C during 20 min, both cysteines reacted rapidly with DTNB (Fig. 8*c*, *curve 2*), suggesting that the accessibilities of Cys-302 and Cys-382 strongly increase in the GAPN* species.

DISCUSSION

Evidence in Favor of the Existence of a Phosphate Binding Equilibrium on GAPN—The DSC analysis of solutions of GAPN in potassium P_i buffers, pH 8.2, showed the presence of two thermally induced transitions A and B of GAPN, characterized by high and low T_{max}, respectively. From native PAGE, gel filtration, and sedimentation experiments, endotherms A and B were assigned to two species of tetrameric GAPN, both unfolding irreversibly on temperature increase. The species corresponding to endotherm B would differ from that of endotherm A by a lower thermostability and a higher electrophoretic mobility due to the presence of 4 mol of phosphate/mol of tetramer. Therefore, endotherm A would represent the thermal unfolding of free GAPN, and endotherm B, the thermal unfolding of the GAPN·phosphate binary complex. This result, obtained by direct phosphate titration on both individual species of the C302A GAPN isolated by native PAGE, was further supported by the dependence of the T_{max} of the thermolabile species on phosphate concentration for the wild-type enzyme, which increases linearly as a function of ln[phosphate] (not shown). Such a behavior suggests that phosphate likely dissociates prior to the rate-determining step of the thermal unfolding process (19), thus implying that this species corresponds to a complex of GAPN with phosphate. For thermostable A species, on the contrary, the T_{max} values decrease for increasing phosphate concentrations, whereas the line shape of the corresponding peak flattens. Furthermore, the effect of high concen-

trations of NaCl on endotherm A in the presence of 20 or 50 mM phosphate is similar to the effect of phosphate at similar ionic strength (Fig. 2). Because these effects are significant only at high concentrations, they are consistent with a thermal destabilization effect due to either an increase of the ionic strength or to a nonspecific binding of phosphate on GAPN.

Analysis of the titration of GAPN by phosphate using DSC showed the increase and decrease of the areas of endotherms B and A, respectively. This behavior suggests that, in the presence of phosphate, before heating, a binding equilibrium exists between GAPN and phosphate. However, as a consequence of the irreversible nature of the mechanisms of thermal denaturation, the ΔH_{cal} values could be affected by effects such as aggregation or phosphate dissociation in addition to the concentration of the B form by itself. Therefore, the data reported in Fig. 1 could not be rigorously exploited to determine a dissociation constant for phosphate. The hypothesis of the existence of a binding equilibrium was further supported by the reversibility of the phenomenon when a GAPN solution in 500 mM potassium P_i was extensively dialyzed against the same buffer at 50 mM. However, the timescales of the experimental approaches that allowed us to identify the free and liganded species of GAPN preclude the observation of relatively fast equilibriums. Indeed, assuming the existence of a fast equilibrium, the thermal denaturation of the GAPN-phosphate (thermolabile) species during the DSC experiment should drive the equilibrium toward the binding of phosphate, preventing the observation of endotherm A (free GAPN). Similarly, the separation of both forms by PAGE should result in a continuous smear between the bands. Yet, both species were resolved by DSC and PAGE, indicating the possibility of a slower equilibrium. The kinetics of the increase of the area of endotherm B for wild-type GAPN in the presence of 500 mM potassium P_i were characterized as a first-order process with a half-time estimated to be ~2 h. Therefore, because the thermal denaturation of both species by DSC was, at most, 30 min apart (for a scan rate of 1 °C/min), a maximum of 15% of free GAPN could potentially be transformed into the liganded form in the course of the experiment. In addition, heating to 55 °C in the DSC apparatus resulted in the transformation of free GAPN into GAPN*, which appeared to be irreversible on the timescale of the experiment, thereby trapping the protein as GAPN* during the thermal scanning (this might also be true during the PAGE separation). However, this transformation could, by itself, drive the equilibrium toward the dissociation of phosphate. Because the kinetics of the decrease of the area of endotherm B in a solution dialyzed from 500 to 4 mM potassium P_i are slow on the timescale of the DSC experiment (half-time of 1.8 h), the endotherm B was expected not to be perturbed by the GAPN→GAPN* process along the DSC experiment. Besides, the kinetics of the thermal unfolding, by themselves, could interfere with the analysis of the equilibrium. However, the timescale of the denaturation, with rates that depend on the temperature and fall into the 3–100-h^{-1} range, from the beginning to the end of the transition peak (according to the analysis as a simple two-state kinetic model), are fast compared with the kinetics of evolution of the area of endotherm B. Consequently, the DSC analysis can almost be considered as a snapshot of the composition in free and phosphate-complexed populations of GAPN in solution. The same rationale likely also applies to the PAGE experiments that are performed on a similar timescale as DSC (<2 h).

On these bases, several lines of evidence argue in favor of an equilibrium of association/dissociation of phosphate to GAPN. First is the fact that the formation of the GAPN·phosphate binary complex specifically depends on the phosphate concentration and not on ionic strength; therefore, the saturation of the dependence of the area of endotherm B on the phosphate concentration, even if it cannot be rigorously exploited to determine a dissociation constant, is another indicator of the existence of an equilibrium. Second is the reversibility of the conversion between both species upon dialysis against lower phosphate concentration and, in addition, the fact that these processes could be followed kinetically in both directions. Third is the demonstration that the C302A mutant of GAPN binds phosphate ions with a defined stoichiometry of 4 mol of phosphate ion/tetramer by direct phosphate determination, a result that can reasonably be extrapolated to the wild type. Such conclusion is also supported by the separation of both species by PAGE, showing a higher electrophoretic mobility for the GAPN·phosphate complex, consistent with the binding of the negatively charged phosphate ion to GAPN and by the dependence of the T_{max} of endotherm B on phosphate concentration.

If other anions than phosphate were able to bind to GAPN, they could thus be compared with phosphate by the DSC technique. As shown in Fig. 7, sulfate can bind to GAPN, contrary to chloride. Qualitatively, from the ΔH_{cal}(B) values, phosphate appears to bind more specifically to GAPN than sulfate. This result again supports the existence of a specific interaction between phosphate and GAPN, because a specific effect is obtained with an ion of similar geometry, *i.e.* sulfate.

The comparison between the kinetics of phosphate dissociation for the wild-type and C302A GAPNs shows that it occurs ~30-fold slower for the mutant. This is probably the reason why the characterization of both species of the C302A GAPN by PAGE was possible in the absence of phosphate. Furthermore, the presence of phosphate in the isolated faster-migrating band of C302A GAPN in these conditions suggests a strong affinity of this mutant for phosphate relative to sulfate, because phosphate remains bound even in the presence of saturated ammonium sulfate concentration in the storage suspension.

Structural Aspects of the Binding—The study of a set of GAPN mutants showed that, only in the thermogram of the R124L GAPN, the peak corresponding to the complex is absent and, only in the native PAGE analysis of this mutant, no significant trace of a band corresponding to the complex is revealed. Because the Arg-124 residue is only involved in the binding of the phosphate group of GAP (9), these observations strongly suggest that it represents the specific site of interaction of phosphate on GAPN. However, this assignment does not provide a clear explanation for the higher apparent affinity of phosphate for C302A GAPN compared with the wild type, although the removal of the negative charge of the Cys-302 thiolate in the mutant could relieve a possible repulsion with the phosphate bound.

If phosphate binds to the C-3 subsite of the GAP binding site, then other specific ligands should be able to bind to this subsite. Previous study shows that GAP behaved as a competitive substrate inhibitor with a K_I of 0.54 mM (3). This indicated that, at high concentration, GAP binds to the apoenzyme, causes a conformational change that closes the active site, and thus prevents NADP from binding. This hypothesis was tested with G3P, a competitive inhibitor of GAP. As shown in Fig. 6*a*, at low potassium P_i concentration, in which the phosphate-complexed population is not significant, the addition of G3P resulted in the emergence of endotherm B, supporting the binding of this analog to the same site as phosphate and as the C-3 phosphate of GAP.

Relevance to the Enzymatic Mechanism—This study describes a very unusual, strong thermal destabilization of GAPN upon phosphate binding. Several arguments support the idea that the above described phenomenon is relevant to the catalytic mechanism. First, phosphate specifically binds into a de-

fined subsite of the substrate binding pocket. Second, the substrate analog G3P also binds to GAPN and generates a GAPN complex with similar thermal behavior as the phosphate complex. Third, a comparable destabilizing effect is observed when NADP (but not NAD) binds to GAPN.[3] Indeed, the addition of increasing concentrations of NADP results in the emergence of an endotherm with a T_{max} value of 42–46 °C (corresponding to the GAPN·NADP complex), shifted by ~25 °C compared with the thermal transition corresponding to the unliganded GAPN (curves not shown). Such large thermal destabilization effects are indicative of structural reorganization events, at least in the active site. Furthermore, thermoinactivation of unliganded GAPN into GAPN* species is not only coupled to a loss of the capability to bind phosphate, but also to a change in the accessibility of the catalytic Cys-302, which must result from an alteration of the structure of the active site.

The requirement of active site reorganization at different steps of the catalytic cycle of ALDHs has already been pointed out from enzymatic and structural studies. As described in the Introduction, one evidence consists in the consequences of the binding of NADP to GAPN and of the formation of the Michaelis ternary complex GAPN·NADP·substrate. The local conformational rearrangement occurring at this stage leads to the activation of Cys-302 and to the optimization of the relative positions of the substrate and catalytic residues Glu-268, Cys-302, and Asn-169 (the latter being an essential part of the oxyanion hole) (4, 5). Other evidence was recently obtained from biochemical and structural studies done on different members of the ALDH family with oxidized and reduced cofactors. Indeed, studies on both human cytosolic and mitochondrial ALDHs have suggested that a conformational isomerization of the nicotinamide moiety of the coenzyme likely occurs during the catalytic cycle. This movement of the cofactor would be a prerequisite for Glu-268 to be in a competent position to act as a base in the hydrolysis of the thioacylenzyme intermediate (6, 7). In addition, recent structural x-ray data on a GAPN ternary complex have convincingly demonstrated the occurrence of the isomerization conformational step as a flip movement of the nicotinamide moiety of the cofactor,[4] strongly suggesting a link between this cofactor flip rearrangement, conformational flexibility of the active site, and thermal destabilization occurring upon substrate and/or cofactor binding. Therefore, on the basis of the present work and of the various studies on different ALDHs, we propose that ligand-induced thermal destabilization is a mechanism that provides to ALDHs the required flexibility for an efficient catalysis.

Acknowledgments—We are indebted to Dr. M. Desmadril for using the DSC apparatus in his laboratory for some experiments, and to Dr. A. Van Dorsselaer for performing mass spectrometry analyses. We are grateful to Dr. S. Azza and S. Boutserin for efficient technical help. We also gratefully acknowledge Prof. N. K. Nagradova for helpful discussions. Circular dichroism experiments and DSC experiments on the VP-DSC apparatus were conducted in the "Service Commun de Biophysicochimie des Interactions Moléculaires" of the University Henri Poincaré Nancy I.

[3] V. Muronetz, unpublished results.

[4] K. D'ambrosio, A. Pailot, F. Talfournier, C. Didierjean, E. Benedetti, A. Aubry, G. Branlant, and C. Corbier, manuscript in preparation.

REFERENCES

1. Habenicht, A. (1997) *Biol. Chem.* **378,** 1413–1419
2. Boyd, D. A., Cvitkovitch, D. G., and Hamilton, I. R. (1995) *J. Bacteriol.* **177,** 2622–2627
3. Marchal, S., Rahuel-Clermont, S., and Branlant, G. (2000) *Biochemistry* **39,** 3327–3335
4. Marchal, S., and Branlant, G. (1999) *Biochemistry* **38,** 12950–12958
5. Cobessi, D., Tete-Favier, F., Marchal, S., Branlant, G., and Aubry, A. (2000) *J. Mol. Biol.* **300,** 141–152
6. Hammen, P. K., Allali-Hassani, A., Hallenga, K., Hurley, T. D., and Weiner, H. (2002) *Biochemistry* **41,** 7156–7168
7. Perez-Miller, S. J., and Hurley, T. D. (2003) *Biochemistry* **42,** 7100–7109
8. Cobessi, D., Tete-Favier, F., Marchal, S., Azza, S., Branlant, G., and Aubry, A. (1999) *J. Mol. Biol.* **290,** 161–173
9. Marchal, S., and Branlant, G. (2002) *J. Biol. Chem.* **277,** 39235–39242
10. Marchal, S. (2001) in *Faculté des Sciences, UFR Sciences et Techniques Biologiques*, pp. 200, Université Henri Poincaré, Nancy, France
11. Zhang, L., Ahvazi, B., Szittner, R., Vrielink, A., and Meighen, E. (1999) *Biochemistry* **38,** 11440–11447
12. Kunkel, T. A., Bebenek, K., and McClary, J. (1991) *Methods Enzymol.* **204,** 125–139
13. Scopes, R. K. (1974) *Anal. Biochem.* **59,** 277–282
14. Levashov, P., Orlov, V., Boschi-Muller, S., Talfournier, F., Asryants, R., Bulatnikov, I., Muronetz, V., Branlant, G., and Nagradova, N. (1999) *Biochim. Biophys. Acta* **1433,** 294–306
15. Roitel, O., Ivinova, O., Muronetz, V., Nagradova, N., and Branlant, G. (2002) *Biochemistry* **41,** 7556–7564
16. Van Veldhoven, P. P., and Mannaerts, G. P. (1987) *Anal. Biochem.* **161,** 45–48
17. Cogan, E. B., Birrell, G. B., and Griffith, O. H. (1999) *Anal. Biochem.* **271,** 29–35
18. Sanchez-Ruiz, J. M., Lopez-Lacomba, J. L., Cortijo, M., and Mateo, P. L. (1988) *Biochemistry* **27,** 1648–1652
19. Sanchez-Ruiz, J. M. (1992) *Biophys. J.* **61,** 921–935
20. Kurganov, B. I., Lyubarev, A. E., Sanchez-Ruiz, J. M., and Shnyrov, V. I. (1997) *Biophys. Chem.* **69,** 125–135

Thermal Destabilization of Non-phosphorylating Glyceraldehyde-3-phosphate Dehydrogenase from *Streptococcus mutans* upon Phosphate Binding in the Active Site

Sophie Rahuel-Clermont, Denis Arutyunov, Stéphane Marchal, Victor Orlov, Vladimir Muronetz and Guy Branlant

J. Biol. Chem. 2005, 280:18590-18597.
doi: 10.1074/jbc.M414110200 originally published online March 9, 2005
